Structural Eng. / Earthquake Eng. Vol. 3. No. 2, 439s-446s. October 1986
Japan Society of Civil Engineers (Proc. of JSCE No. 374/I-6)

SEISMIC RESPONSE ANALYSIS OF PIPELINES BURIED IN SOIL LAYERS WITH IRREGULAR BOUNDARIES

By Takashi AKIYOSHI, Kunihiko FUCHIDA** and Kazuhisa MATSUMOTO****

Analysis of seismic response of pipelines buried in surface layer with irregular boundaries is presented here. A soil layer model which consists of two-dimensional upper and lower layers is solved by using the boundary element method for SH-type earthquakes. For the excitation of surrounding soil, strain and joint expansion of pipes under imperfect bonding at soil-pipe interface are analyzed. Results show that proposed method is fairly proper to express the phenomenon of strain concentration at the joints of pipes and a conventional aseismic design guideline overestimates the strain of slipped pipe for irregularly bounded layers.
Keyword : pipeline, seismic response, slippage

1. INTRODUCTION

It may be noted from the observations of seismic damages that most of pipeline failures have occurred at the joints in poor soils or near irregular boundaries of soil layers. So much effort has been devoted to the investigations of buried pipeline response to earthquakes and establishment of effective aseismic design procedures. However seismic damages of pipelines do not seem to decrease yet, as has been seen in recent earthquakes, Miyagikenoki earthquake (1978) and Nihonkai-chubu earthquake (1983). Hence to stimulate understanding on the mechanism of pipeline damages, presentation of a reasonable soil-pipe model to express the strain concentration at the joints is required.

With respect to the effect of irregularity of soil boundary on the seismic response, most of works have been achieved by using the conventional numerical procedures, finite element method (FEM) and boundary element method (BEM)[1)~4)]. Regarding pipe response embedded in a soil layer, two different approaches have been taken according to the definition of surrounding soil. One is based on the use of spring constant of soil which is usually decided empirically and therefore cannot describe the dynamic characteristics of soil deposite[5)]. Another is based on coupling between pipe and spatial soil which is mostly processed by FEM or BEM for sinusoidal excitation[6)~16)]. However so far adjustment of the results by both approaches does not seem to be successful.

This paper which is basically on the latter approach and the extension of our previous works[11),12)] aimes to investigate the effect of irregularity of soil boundaries on the seismic response of pipelines and present a rough estimation of the strain and joint expansion. Results obtained are compared with the guideline for

* Member of JSCE, Dr. Eng., Professor, Dept. of Civil Eng., Kumamoto Univ.
** Member of JSCE, Research Associate, Dept. of Civil & Arch. Eng., Yatsushiro College of Technology.
*** M. Eng., Ohbayashi-gumi Ltd., Formerly Graduate Student, Dept. of Civil Eng., Kumamoto Univ.

aseismic design of gas pipeline for normalized El Centro earthquake (1940)[17]. Analysis is performed based on the dynamic coupling of an infinite soil layer and pipelines through the frictional interface.

2. GENERAL FORMULATION

In this study two-dimensional elastic soil layer model which is subjected to SH-type earthquakes is used as shown in Fig. 1 in which V_1, V_2 are shear wave velocities of surface and base layer, respectively, and H_1, H_2 are thickness of side (thin) and central (thick) area, respectively. Further the surface layer is assumed to have hysteretic damping and irregular boundary areas in which "irregularity" is defined as dipping of boundary planes.

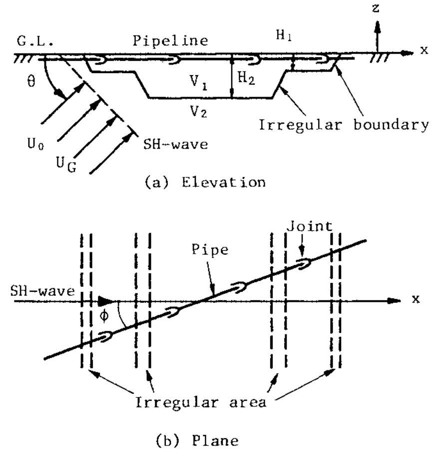

Fig. 1 Geometry of soil layer and pipeline.

Using BEM, equation of motion of surface layer under steady harmonic vibration is formulated in the matrix form (the detail is shown in reference 1)).

$$K^*U^*=P^* \quad \cdots\cdots (1)$$

in which K^*, U^*, P^* are respectively stiffness matrix, displacement and traction vectors for all boundary elements of the system.

Then equation of motion for scattered wave also takes the form

$$K_R U_R = P_R \quad \cdots\cdots (2)$$

in which K_R is stiffness matrix, and U_R, P_R displacement and traction vectors of waves scattered at the surface-base layer interface.

In this case, boundary conditions at the interface for input displacement U_0 and traction vectors P_0 are written by

$$\left.\begin{array}{l} U_I = U_R + U_0 \\ P_I + P_R + P_0 = 0 \end{array}\right\} \quad \cdots\cdots (3)$$

in which U_I, P_I are respectively displacement and traction vectors at the interface. Eliminating P_I from eqs. (1)~(3) yields

$$\begin{bmatrix} K_{II}+K_R & K_{IS} \\ K_{SI} & K_{SS} \end{bmatrix} \begin{Bmatrix} U_I \\ U_S \end{Bmatrix} = \begin{Bmatrix} K_R U_0 - P_0 \\ P_S \end{Bmatrix} \quad \cdots\cdots (4)$$

in which U_S, P_S are displacement and traction vectors at the ground surface and therefore $(U_I,\ U_S) = U^*$.

When a plane harmonic SH-wave of unit amplitude travels in a half space, U_0 takes the form

$$U_0 = 2\cos(\omega z \sin\theta / V_2)\exp[i\omega(t - x\cos\theta / V_2)] \quad \cdots\cdots (5)$$

in which ω is circular frequency, θ incident angle of SH-wave measured from horizontal plane, and x, z respectively horizontal and vertical (upward is positive) coordinates. Traction P_0 at the interface of both layers is also obtained using eq. (5).

Thus displacements U_I and U_S which are solved by substituting U_0 and P_0 into eq. (4) become frequency response functions (FRF) of displacement to displacement conversion type. Now let $H_S(\omega)$ be FRF of the ground surface. Then for a SH-type earthquake $U_G(t)$, spectral displacement amplitude $U_S(\omega)$ of ground surface becomes

$$U_S(\omega) = H_S(\omega)\, U_G(\omega) \quad \cdots\cdots (6)$$

in which $U_G(\omega)$ is Fourier transform of displacement $U_G(t)$ of an earthquake at the interface. Here an example of $|U_S(f)|$ for El Centro earthquake (1940) is shown in Fig. 2 with white circles.

Next the concept of seismic response analysis of buried pipelines may be stated below, in which pipelines are assumed to be periodically jointed as shown in Fig. 1 and treated as a statically equivalent uniform one through the study (see references 11) and 12) if the detail is necessary).

First step must begin with slip check of a pipe for the spectral displacement amplitude $U_S(\omega)$ of surrounding soil, which means to determine the slip amplitude $U(\omega)$ because FRF of buried pipeline depends on $U(\omega)$. Fig. 2 also shows $|U(f)|$ by asterisks along with the critical slip amplitude U_{cr} (solid line). If $|U_S| < U_{cr}$, slip does not occur and therefore $U=0$ which is shown on the frequency axis. However, if $|U_S| > |U_{cr}|$, slip takes place and U is computed from the equation of soil-pipe interaction as the plots in Fig. 2 with asterisks over U_{cr}. The diagram denotes that slip become perfect when $|U_S| \gg U_{cr}$, and imperfect when $|U_S|$ is close to U_{cr}. Thus employing FRF $H_P(\omega)$ of a pipeline which can be determined based on coupling with surrounding soil, spectral displacement amplitude $U_P(\omega)$ of the pipeline may take the form

$$U_P(\omega)=H_P(\omega)\,U_S(\omega)=H_P(\omega)\,H_S(\omega)\,U_G(\omega) \quad \cdots\cdots\cdots\cdots (7)$$

Strain $\varepsilon_P(\omega)$ of pipeline is also obtained by taking similar process which leads to

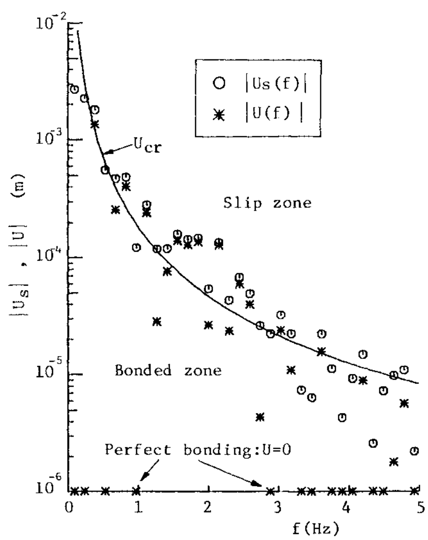

Fig. 2 Spectral displacement amplitudes $|U(f)|$, $|U_s(f)|$ and critical slip amplitude U_{cr}.

$$\varepsilon_P(\omega)=G_P(\omega)\,U_S(\omega)=G_P(\omega)\,H_S(\omega)\,U_G(\omega) \quad \cdots\cdots\cdots\cdots (8)$$

in which $G_P(\omega)$ is FRF of pipe strain.

Thus finally root mean square (RMS) strain and joint expansion of pipeline are evaluated directly from eqs. (7) and (8), and time-historic response from inverse Fourier transform of those equations.

3. NUMERICAL RESULTS

Standard values of the parameters of earthquakes, soils and pipes used for numerical computations are as follows; shear wave velocity of surface and base layer are respectively $V_1=100$ m/s and $V_2=400$ m/s, thickness of thin (both-sided) and thick area of surface layer respectively $H_1=20$ m and $H_2=70$ m, bottom length of thin and thick area respectively 0.5 km and 1.0 km, horizontal incident angle to pipe $\phi=45°$, hysteretic damping constant=20 %, ratio of frictional slip stress to shear modulus of soil $\bar{\tau}_S=\tau_S/G=10^{-4}$, radius of pipe $r_0=0.3$ m, wave velocity of pipe $V_P=4$ km/s, and maximum acceleration of reference earthquake [=El Centro earthquake (1940)], $A_{max}=100$ gal, in the base layer.

Fig. 3 shows an example of the distribution of FRF at resonance for incident angle (a) $\theta=0°$ and (b) $\theta=45°$ in which solid line is the plot for $f=0.390$ Hz and broken line for $f=1.025$ Hz. Both figures show that irregular boundary areas induce sharp strain concentration at low frequency range and have low resonant frequencies.

Fig. 4 describes the response wave forms of shear strains at the ground surface subjected to El Centro earthquake (1940) in which (a) and (b) are respectively the cases of $\theta=0°$ and $45°$, and (c) is the case of $V_1=200$ m/s ($\theta=0°$). The diagrams (a) and (b) denote that thin layer transfers rather high frequency components of small amplitudes, but thick layer generates surface wave of large amplitude. Irregular (dipping) boundary area produces more complicated and high frequency-dominated waves. However harder surface layer ($V_1=200$ m/s) does not seem to induce surface wave as shown in the diagram (c). Thus buried pipeline which depends mostly on surrounding soil strain may suffer from earthquakes at the irregular boundary area and thick area of surface layer.

In Fig. 5, solid lines denote the theoretical phase velocity curves of Love waves of fundamental mode, broken lines the apparent wave velocity of SH-wave and the dots the dominant wave velocities which are roughly read from time-distance curves in Fig. 4. The dominant wave velocity in a thick layer (white dots : $H=70$ m) is close to Love wave one in the period of 2 to 3 seconds. However in a thin layer (black dots : H

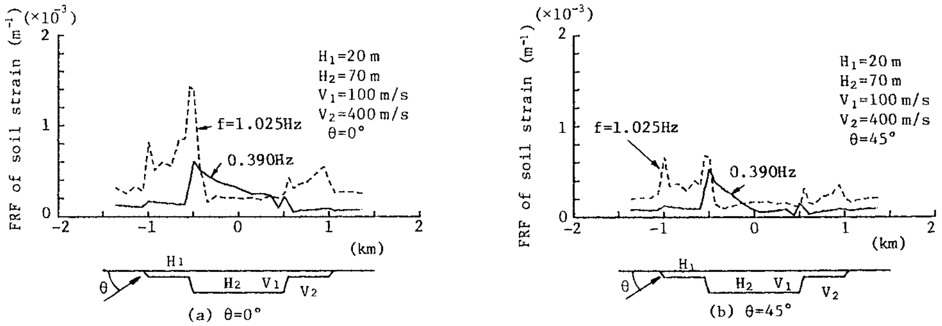

Fig. 3 Distribution of FRF of surface soil strain.

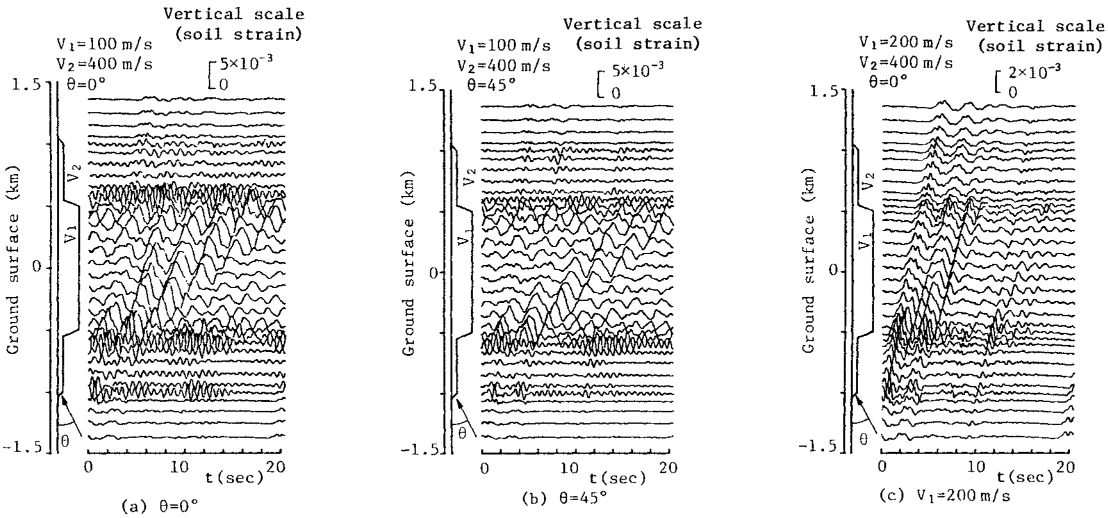

Fig. 4 Wave forms of soil strains on the ground surface.

=20 m), dominant wave velocities approach the apparent ones of SH-wave with the period of about 0.8 seconds which coincides with theoretical period $T=4\,H/V_1=0.8$ seconds. Thus it can be noted that body wave dominates in thin or hard layer and surface wave in thick or soft layer.

Soil strain at the ground surface, which will be shown in Figs. 6 and 7, is important as the input to pipelines. Fig. 6 is the diagram of the distribution of root mean square (RMS) strain of soil at the ground surface for a horizontal input. High strain concentration is induced at the irregular (dipping) area for soft soil. This may mainly come from local accumulation of vibrational energy flow at the irregular area. Soil strain distributions are also plotted in Fig. 7 for three incident angles. Horizontal propagation of earthquakes not only gives sharpest strain concentration on irregular areas, especially at the transition area of thin to thick layer, but also raise the strain of the central area of the surface layer.

For the excitation of surrounding soil, RMS distribution of strain and joint expansion of pipe are plotted in Figs. 8 and 9 for various slip stresses in which the diagrams (a) and (b) are the case of $\theta=0^\circ$ and 90°, respectively. As shown in Fig. 8 (a), horizontal propagation ($\theta=0^\circ$) yields not only a local concentration of pipe strain at the irregular area but also high-level strain distribution even on the central area of the surface layer, but small slip stress releases it because of slippage. However vertical propagation ($\theta=90^\circ$) gives rather smaller strain concentration to pipe and holds the spatial distribution form even for small slip stress ($\bar{\tau}_S=10^{-6}$) as shown in Fig. 8 (b).

Fig. 9 (a) and (b), however, describe increase of joint expansion of pipe with decreasing τ_S. Thus the relation between pipe strain and joint expansion is complementary.

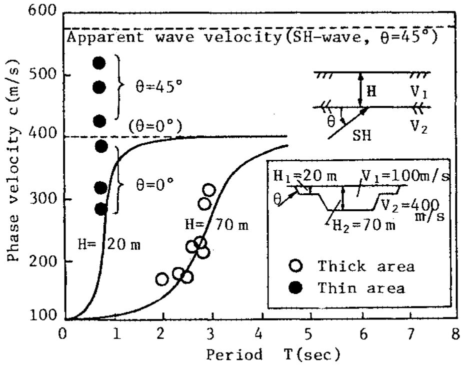

Fig. 5 Phase velocity of Love wave in two soil layers.

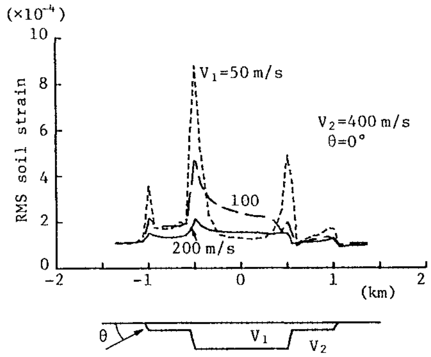

Fig. 6 Distribution of RMS soil strain.

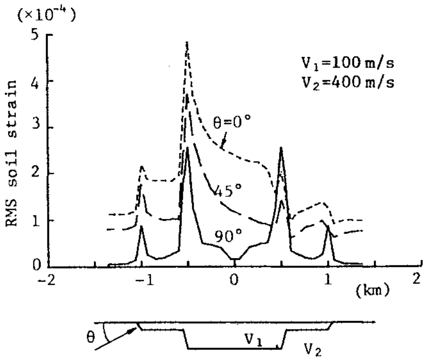

Fig. 7 Distribution of RMS soil strain.

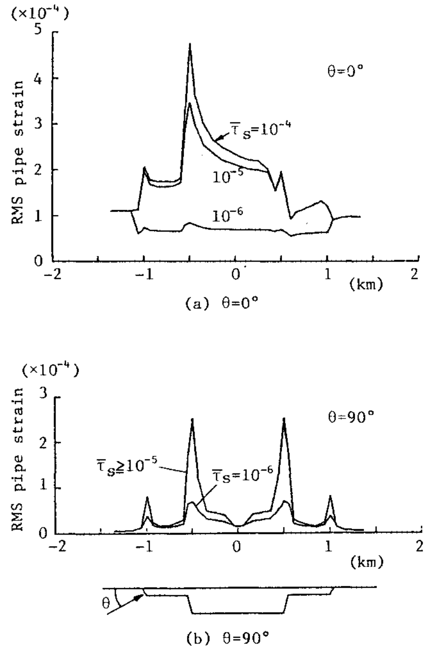

Fig. 8 Distribution of RMS pipe strain.

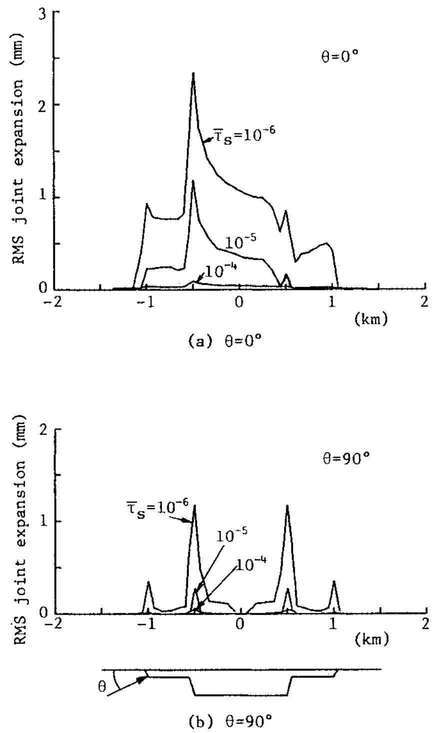

Fig. 9 Distribution of RMS joint expansion.

Now compare the pipe strain by proposed method with the guideline for aseismic design of gas pipelines[17], partially using the method of M. Shinozuka and T. Koike[13),14)]. According to the guideline, soil displacement and strain in a surface layer with parallel boundary are basically derived by horizontal seismic coefficient and natural period $T=4H/V_1$ (H : thickness, V_1 : shear wave velocity of surface layer). This procedure also applies irregular boundary area in which H is replaced with the depth to dipping plane. Fig. 10 (a) and (b) are the diagrams of pipe strain embedded in a soil layer respectively for the cases of surface layer with parallel boundary and irregular (dipping) boundary in which solid line denotes the guideline and symbolic marks maximum pipe strain by proposed method. The diagram (a) shows that proposed pipe strains slightly exceed the guideline for $\bar{\tau}_S=\tau_S/G=10^{-4}\sim10^{-5}$, but are less than that for $\bar{\tau}_S=10^{-6}$. There is not much difference between both methods for the soil layers with parallel boundaries, because $\bar{\tau}_S$ is expected to be by and large 10^{-5} according to laboratory tests[17]. Further the diagram (b) denotes that, for irregularly bounded area, the guideline may provide comparable estimate of pipe strain for nearly bonding case ($\bar{\tau}_S=10^{-4}\sim10^{-5}$), but overestimate for slipping case ($\bar{\tau}_S=10^{-6}$).

From practical view point, it may be important to present the seismic response curve of pipe strain and joint expansion in terms of slip stress τ_S and pipe length l, as shown in Figs. 11 and 12 in which solid and broken lines show respectively the cases for No. 1 point (irregular boundary area) and No. 2 point of observation (center of parallel boundary area). Fig. 11 denotes that there exists a critical slip stress $\bar{\tau}_{cr}=$

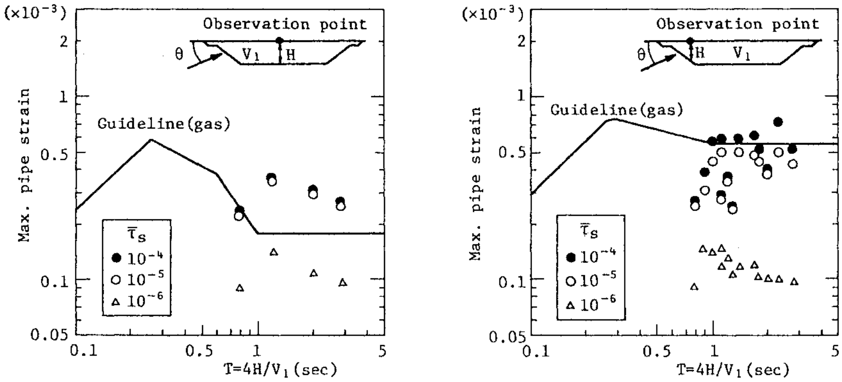

(a) For parallel boundary area (b) For irregular boundary area

Fig. 10 Comparison of proposed pipe strain (Max.) with a guideline (gas).

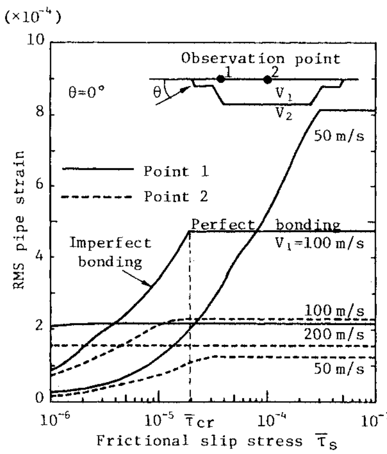

Fig. 11 RMS pipe strain versus frictional slip stress.

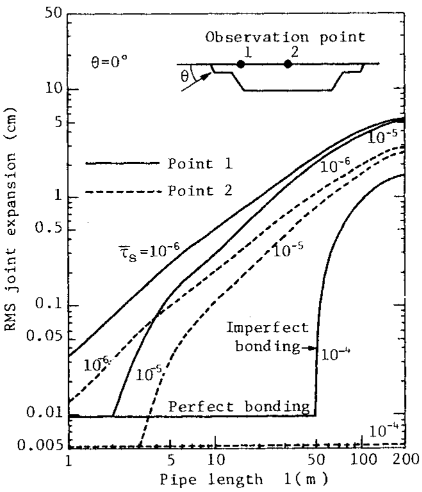

Fig. 12 RMS joint expansion versus pipe length.

τ_{cr}/G as the breaking point on pipe strain-slip stress curve which increases with decreasing shear wave velocity V_1 of surface layer, and soft soil (small V_1) is easy to enter the imperfact bonding state which releases pipe strain. Also the diagram implies that pipe strain in perfect bonding state varies approximately in inverse proportion to V_1 and is amplified at irregular boundary area, but is not so dependent on V_1 at the central point of parallel boundary area as already shown in Fig. 6. However one of essential factors to cause seismic damages of pipelines may be excessive joint expansion which is defined as the accumulation of released pipe strain during slippage plus relative displacement of a joint under perfect bonding state which is usually negligibly small. Amplification effect of joint expansion by irregular boundary also appears in Fig. 12. Long pipe generates large joint expansion by slippage which may be fatal to many joints except for mechanical ones. However joint expansion of standard size pipe (length l=5 meters) is so small (less than 0.2 cm in the diagram) that, though it may be still destructive to screw or flange-type joints, it is absorbable to usual mechanical ones. Thus the figure recommends dense attaching of joints at irregular boundary area because short length pipe is effective to prevent slippage and accumulation of strain at joint.

4. CONCLUSION

Firstly the response of irregularly bounded soil layers during earthquakes have been investigated using the boundary element method. Then strain and joint expansion for the excitation of surrounding soil are analyzed basically depending on our previously presented procedures. Results obtained are summarized as follows :

(1) Proposed method is effective to express stress concentraion at the pipe joints by slippage during earthquakes.

(2) Surface layer induces high strain concentration at the irregularly bounded area and for horizontal propagation of earthquakes, and further generates srface wave in the thick area.

(3) Pipe strain follows soil strain in hard soil, but is released by slippage in soft soil.

(4) Small slip stress releases pipe strain by slippage.

(5) Proposed pipe strain is comparable with a conventional guideline for aseismic design of gas pipelines for parallel boundary layer. For irregularly bounded layer, the guideline overestimates pipe strain, compared with proposed method for the case of slippage.

(6) At irregular boundary area, dense attaching of joints is recommended to prevent strain accumulation by slippage.

REFERENCES

1) Toki, K. and Sato, T. : Seismic Response Analyses of Ground with Irregular Profiles by the Boundary Element Method, Natural Disaster Science, Vol. 5, No. 1, pp. 31~52, 1983.

2) Ohtsuki, A. and Harumi, K. : Effect of Topography and Subsurface Inhomogeneities on Seismic SV Waves, Int. J. Earthq. Eng. Struct. Dyn., Vol. 11, pp. 441~462, 1983.

3) Ohtsuki, A., Tazoh, T. and Shimizu, K. : Effect of Lateral Inhomogeneity on Seismic Waves and Ground strains, Proc. JSCE, Vol. 350, I–2, pp. 291~300, 1984 (in Japanese).

4) Niwa, Y. and Hiroshe, S. : Theoretical Analysis of Seismic Waves in a Dipping Layer, Proc. JSCE, Vol. 337, pp. 57~66, 1983 (in Japanese).

5) Takada, S. : Seismic Response Analysis of Buried PVC and Ductile Iron Pipelines, Proc. Pressure Vessel and Piping Conf., ASME, pp. 23–32, 1980.

6) Goto, H., Shibata, T., Toki, K., Takada, S. and Sunami, S. : Vibrational Characteristics of Pipe Structures in the Near-Surface Ground of Which Physical Properties Vary Spatially, Annuals Disas. Prev. Res. Inst., Kyoto Univ., Vol. 16 B, pp. 631~655, 1973 (in Japanese).

7) Toki, K. and Takada, S. : Earthquake Response Analysis of Underground Tubular Structure, Bull. Disas. Prev. Res. Inst., Kyoto Univ., Vol. 24, Part 2, No. 221, pp. 107~125, 1974.

8) Ugai, K. and Yamaguchi, H. : A Theoretical Study on the Dynamic Modulus of Earth Reaction for Buried Pipe, J. JSSMFE,

Vol. 19, No. 4, pp. 93~102, 1979 (in Japanese).
9) Ugai, K. : Dynamic Analysis of Underground Pipelines under the Condition of Axial Sliding, Proc. JSCE, Vol. 272, pp. 27~37, 1978 (in Japanese).
10) Parnes, R. and Weidlinger, P. : Dynamic Interaction of an Embedded Cylindrical rod under Axial Harmonic Forces, Int. J. Solids Struct., Vol. 17, pp. 903~913, 1981.
11) Akiyoshi, T. and Fuchida, K. : Soil-Pipeline Interaction Through a Frictional Interface During Earthquakes, Int. J. Soil Dyn. Earthq. Eng., Vol. 3, No. 1, pp. 27~34, 1984.
12) Akiyoshi, T. and Fuchida, K. : Effect of Slippage on the Seismic Response of Buried Pipes, Proc, JSCE, Vol. 334, pp. 25~34, 1983 (in Japanese).
13) Shinozuka, M. and Koike, T. : Estimation of Structural Strains in Underground Lifeline Pipes, Lifel. Earthq. Eng.-Buried Pipel., Seism. Risk, and Instrum., ASME, pp. 31~48, 1979.
14) Koike, T. : Estimasion of Buried Pipe Strains Under Seismic Risk, Proc. JSCE, Vol. 331, pp. 13~24, 1983 (in Japanese).
15) Satake, M., Kishino, Y. and Asano, T. : Considerations on Earthquake Resistance of Pipeline Buried in Non-Uniform Ground, Proc. 6 th Japan Earthq. Eng. Symp., pp. 1905~1912 (in Japanese).
16) Ohishi, H. and Sekiguchi, K. : Considerations on Strain-Occurance Mechanism of Underground Pipelines During Earthquake, Proc. JSCE, Vol. 350, I-2, pp. 227~236, 1984 (in Japanese).
17) Japan Gas Association : Guideline for Seismic Design of Gas Pipeline, pp. 21~67, pp. 78~217., 1982 (in Japanese).

(Received February 20 1986)